Higher Drawing Depth and Less Wrinkling Due to Drawbeads in Paperboard Forming

Nicola Jessen and Peter Groche *

Deep drawing of paperboard has shown promising results for the packaging industry due to its high productivity, economical process routes, and geometrical freedom. Paper, as a material, offers a combination of compostability and recyclability while consisting of renewable resources. However, formed paper can exhibit wrinkles due to the excess material during the deep drawing process. Wrinkles form differently depending on the anisotropic behavior caused by fiber orientations. To control material deformation while forming asymmetric components the sheet metal industry uses draw beads. This paper investigates the impact of draw beads on paperboard forming. The goal is to avoid additional process steps while increasing the achievable drawing depth as well as the wrinkle control. The design of the draw beads, including their advantages and disadvantages, is discussed based on experimental tests and compared with numerical simulations. Results show that while draw beads increase drawing depth and reduce wrinkles, their position and length affect the severity and distribution of wrinkles, as well as the wrinkle-free distance.

DOI: 10.15376/biores.20.1.1399-1412

Keywords: Deep Drawing; Paperboard; Draw Beads; Modelling; Anisotropy; Wrinkling

Contact information: Institute for Production Engineering and Forming Machines - PtU, Technical University Darmstadt, Otto-Berndt-Straße 2, 64287 Darmstadt, Germany;
** Corresponding author: groche@ptu.tu-darmstadt.de*

INTRODUCTION

In 2022, the European Union published a proposal requiring all member states to reduce packaging waste by increasing re-usage and recycling (Directorate General for Environment 2022). With this proposal, the EU is tackling one of the most discussed topics in the field of climate change. Packaging waste shows an easily relatable and visible problem in society. In 2021, 71.4% of paper in Europe was recycled (European Paper Recycling Council 2021) while only 39.7% of plastic was recycled (Two Sides 2020) in the same year. This is one of the many reasons why the perception of plastic packaging is worse than the perception of paper packaging in an environmental context. Furthermore, a study on “European Packaging Preferences” in 2020 showed that paper packaging is the most valued by consumers in terms of sustainability. The importance of environmentally friendly packaging in today’s society was shown in the same study. It revealed that 70% of European consumers take steps to actively reduce their use of paper packaging. Finally, 48% of consumers avoid retailers that are not trying to reduce their use of plastic packaging, and 44% are willing to spend more on a product if it is packaged in sustainable materials. This highlights the growing consumer demand for sustainable packaging solutions and underscores the urgency for research in this area.

To make paper packaging even more eco-friendly, the production processes must also be as sustainable as possible. This means that the processes should have low material waste, high production rates, low energy consumption, and adaptable tools to produce different geometries. These attributes are well suited to deep drawing processes, which are extensively applied in sheet metal forming. In recent years, deep drawing has been increasingly and successfully tested and implemented with paper. However, the process is not yet as thoroughly researched and detailed as it is for sheet metals. Adapting these processes to paperboard packaging can significantly enhance its environmental benefits, making it a prime focus of current packaging research. Research on the different parameters affecting the product, as well as the parameters that change the outcome is ongoing. Changes in process parameters oftentimes correlate with trade-offs or constraints, for example between process times and achievable drawing depth (Lev *et al.* 2023).

Adapting the deep drawing process to paperboard has created many new challenges (Hauptmann *et al.* 2016). Those challenges relate to the geometric accuracy of the formed shapes as well as the achievable drawing depth. The drawing depth influences the packaging volume and the wrinkle formation. The excess material increases in direct proportion to the drawing depth and, in conjunction with a lack of plastic thickening of paperboard, causes wrinkling. These process characteristics can be ascribed to the material behavior of paperboard. As the fiber material is produced by drying the components on a moving web, the fibers mostly align themselves parallel to the moving direction, with the streamline in machine direction (MD). A smaller amount is directed perpendicular to the moving direction, in cross direction (CD), while some fibers are also directed in z-direction or any direction in between (Visthal and Retulainen 2012).

The specified fiber distribution in the material results in direction-dependent properties, as shown in Fig. 1. The stress strain curves show the differences in material behavior in a tensile test between MD and, in a 90° angle to this, CD. The picture on the right depicts the anisotropic springback after the deep drawing process. Both geometries were formed with the same tool, from the same material and the same process parameters, with the only difference being the fiber orientation. For most papers, improved formability can be observed at an angle of 90°, resulting in the need to choose the paper orientation depending on the anticipated forming (Safwa *et al.* 2024).

Due to the anisotropic distribution of the natural fibers in paperboard and their sensitivity to moisture content and temperature, the anisotropy is also influenced by these ambient parameters (Garat *et al.* 2020). The influence of increased moisture content can also be seen in the stress-strain graph of the investigated paper board in Fig. 1, as it shows a higher strain at 15% moisture content.

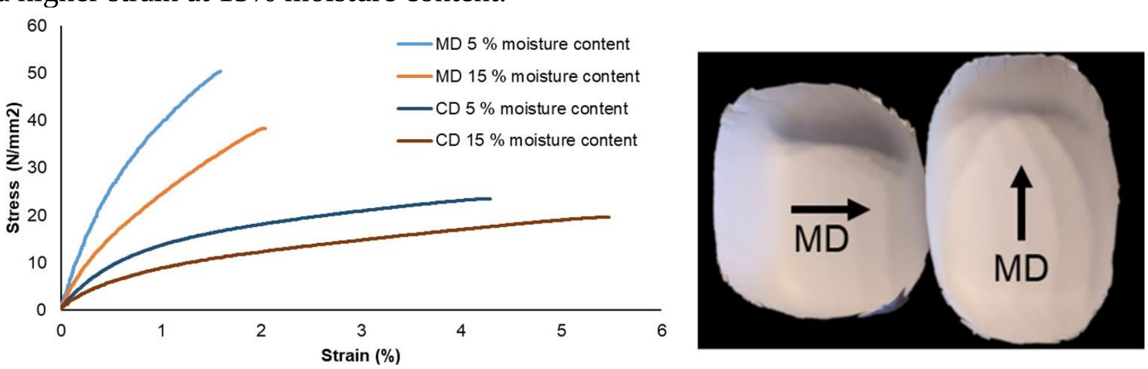

Fig. 1. Moisture content dependent stress strain curve (left) and anisotropic springback (right)

In sheet metal forming, draw beads have proven beneficial when complex, non-symmetrical geometries have to be formed in deep drawing processes. Additionally, draw beads have been shown to prevent the occurrence of wrinkles in the deep drawing of aluminum (Hussein *et al.* 2020). The paper at hand answers the question of whether these experiences can be transferred to paperboard forming.

In order to obtain meaningful results, numerical and experimental results were compared and analyzed. The experimental setup had a high degree of flexibility to investigate different geometries and positions of the draw beads. Results showed a good agreement between numerical and experimental setups, also determining how the position and geometry of the draw beads change the wrinkle formation as well as the draw depth. Overall, the use of draw beads in the deep drawing of paperboard showed improved process control and extended process windows for both draw depth and wrinkle-free areas.

EXPERIMENTAL

The material used in the experiments and numerical simulations was the uncoated bleached tray board, a virgin fiber material, from the manufacturer Stora Enso called Trayforma™ with a grammage of 190 g/m^2 and a thickness of 255 µm. It consists of three layers, with the middle one being chemi-thermomechanical pulp while the outer layers are sulphate pulp. Given its established use in the packaging industry, its suitability for this study is ensured.

To evaluate the mechanical properties of this material, tensile tests were conducted, and the resulting stress-strain graph is shown in Fig. 1. Tensile tests were carried out according to the DIN EN ISO 5270 standard, with modifications to the specimen geometry as suggested by Huttel for better stress homogenization (Huttel 2015). Results are used to define necessary and beneficial material preparations for the deep drawing tests. In these tests, different bead geometries and positions were evaluated and compared to paperboard deep drawn without any draw beads.

Material Preparation

The highest strain was measured at 15% board moisture content. This was determined to be the optimum moisture content for forming, and all experiments were conducted at this moisture content. The moisture conditioning is performed according to DIN EN ISO 287 by first determining the dry weight at 0% moisture and then adding the required amount of moisture. The samples are then stored in a gas-tight container for 24 hours to allow the moisture to homogenize over the samples before they are used in the experiments.

Geometry

The product geometry selected for this study was a tray with a rectangular base measuring 125 mm x 85 mm and corner radii of 20 mm. This geometry is based on commercially available packaging for frozen ready meals and products such as margarine or cream cheese. It is also important to examine two edges of different lengths in order to examine wrinkle-free areas and how draw beads influence their length. The geometry of the deep drawing pre-cut design is based on experience from previous trials and literature (Papadia *et al.* 2010).

Deep Drawing

The deep drawing process employed corresponds to a process with a moving punch in accordance with DIN 8584. The drawing gap between the punch and the die is designed to be 0.3 mm. To accommodate the developing wrinkles, the punch narrows upwards at an angle of 89°. As the drawing depth increases, so does the drawing gap. The deep drawing tool consists of five functional elements: a punch, a drawing die, a two-parted blank holder, a blank holder insert with draw beads and a drawing die insert with the counterpart of the draw beads. The inserts can be exchanged according to the required bead geometry and positioning. Figure 2 illustrates the tool.

It has been demonstrated previously that the blank holder force should be reduced during the drawing process (Wallmeier *et al.* 2016). The press utilized in this study is a single acting press. Compression springs are used to regulate the blank holder force, allowing it to be adjusted at the beginning of the process. Nevertheless, a decreasing blank holder force is not implemented. All test results are compared for different bead geometries using the same experimental setup.

The deep drawing tool consists of additively manufactured elements, allowing for economical and quick adjustments of the tool and draw bead geometry over the course of the investigation.

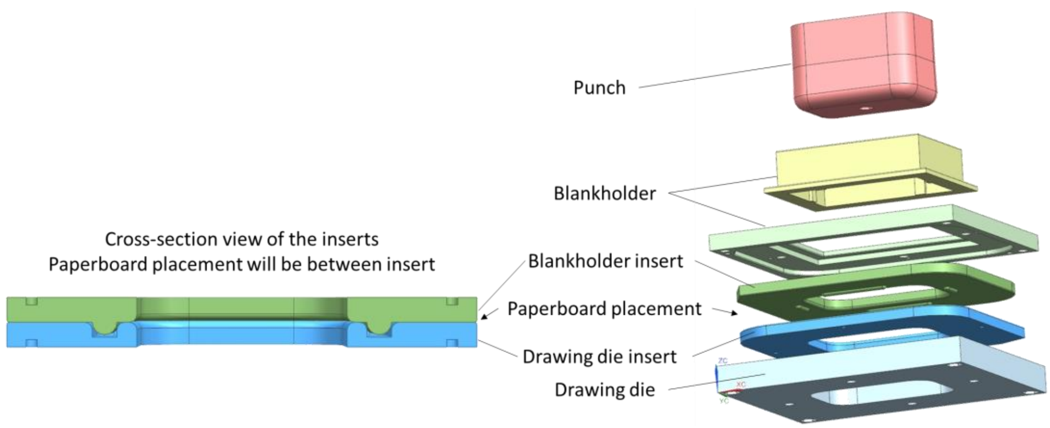

Fig. 2. Deep drawing tool

Draw Beads

The experiments were conducted with six different inserts in the drawing die and blank holder. The insert of the drawing die formed the negative of the insert of the blank holder enlarged by the thickness of the material. All draw beads had a semicircular cross-section, as rectangular cross sections of metal blanks have been shown to result in higher thickness reduction which favors breakage of the specimen (Murali *et al.* 2010).

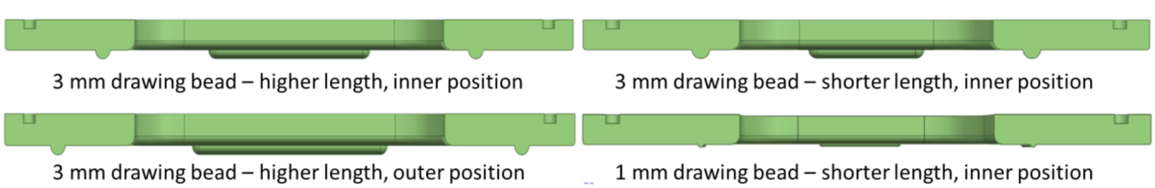

Fig. 3. Different draw bead geometries in the blank holder insert cross section view

The inserts differed with respect to the radius, position, and length of the draw beads, as illustrated in Fig. 3. Those geometric aspects have a high impact on the results, as they define the effectiveness to restrain the material flow (Murali *et al.* 2010). This investigation aimed to determine whether the draw bead would exert a significant influence on the process result only at the beginning of the process or throughout the entire process. The length of the draw bead was either the same length as the edge, up to the beginning of the corner radii (79 mm) or designed according to VDI 3141. This corresponds to an extension of the rounding of the corners by 10° to define the start and end point of the draw bead (65.5 mm). The design according to VDI 3141, thus, leads to shorter draw beads.

Insert 0 represents an insert without a draw bead. Baseline tests were conducted with this insert. Insert 1 (Fig. 3, upper right) had a draw bead radius of 3 mm. The positioning was proximate to the inlet edge (10 mm away), and the draw bead was 65.6 mm long. Inserts 2, 3, 4 and 5 each deviated from geometry 1 in one parameter. Geometry 2 had a radius of 2 mm, geometry 3 had a length of 79 mm (upper left), and geometry 4 (lower left) had a distance of 30 mm to the drawing gap. Geometry 5 (lower right) had a draw bead with a radius of only 1 mm. By varying one parameter at a time, the effect of each could be analyzed and described.

Evaluation Parameters

Starting with the baseline geometry 0, the test series was conducted with all inserts under identical conditions. All tests were conducted five times. The tests were analyzed based on geometric measurements and visual inspections (Wallmeier *et al*. 2014). Samples were examined to determine the number of wrinkles, the achieved drawing depth and wrinkle-free distances. Measurements were conducted using both a caliper gauge and a “Smartzoom 5” digital microscope. A low number of wrinkles, a long wrinkle-free distance, a high drawing depth and a high material elongation are considered beneficial in the scope of this analysis.

NUMERICAL ANALYSIS

Numerical investigations are an essential part of sheet metal forming process design. However, the simulation of processes involving paperboard presents new challenges. Due to the strong individual fluctuation of inhomogeneity, anisotropy, and composition of paper, which are mostly unknown, there are many uncertainties and assumptions in the numerical simulation models. In addition, paper consists largely of natural fibers, which in themselves have a high degree of uncertainty.

Nevertheless, numerical studies of paper have been performed in the past (Jessen *et al.* 2022). Up to now, however, the results have often been qualitative. This is due to the fact that very small numerical elements would have to be used to correctly simulate the wrinkles, and the position of the individual fibers, as well as the position and size of the pores would have to be known. Nevertheless, simulations can help to make predictions and to limit the experimental testing space.

Numerical model

The model used is similar to the setup published in Jessen *et al.* (2022). Since the chosen geometry is axisymmetric, only a quarter of the model was simulated. To model the elasticity of paper as an anisotropic material, orthotropic models were used. The behavior can be described by defining three main directional values for Young’s modulus, Poisson's ratio and shear modulus (Pfeiffer and Kolling 2019). The values were obtained from tensile tests in MD, CD, and 45° direction, while the values in z-direction were calculated following Huang´s approach (Huang and Nygårds 2010).

To correctly describe material behavior for forming simulations, plasticity must also be considered. To build this part of the model tensile test results were implemented again. The anisotropic behavior was modelled according to Hill using the yield and creep stress ratios, which were calculated using yield strengths and a reference stress. The process and material boundaries were determined by the "displacement at failure" method, which calculates the occurrence of fractures from values such as elongation at break and tensile strength (Huttel 2015). These values were obtained from both tensile and cupping tests, as the latter includes the directional dependency of the different parameters.

Friction was implemented using Columb's law of friction. For this purpose, the coefficient of friction between the punch and the paper blank was defined as $\mu_R = 0.3$. The remaining friction coefficients were set to $\mu_R = 0.05$. Values were obtained by comparing numerical results with experimental tests and literature (Huttel 2015).

The model was validated by the simulation of tensile tests and their accordance to the experimental tensile test results (Jessen *et al.* 2022). Although the obtained results were satisfactory, the necessary assumptions regarding the individual fibers and pores resulted in shortcomings, for example, in the numerical wrinkle representation. Relevant values of the material model can be found in Table 1.

Table 1. Values of the Material Model

Density [t/mm^3]		7.1 x 10^{-10}	Thickness [mm]		0.255	Moisture content [%]		15
Elasticity								
Young´s modulus [N/mm^2]			Poisson´s ratio [-]			Shear modulus [N/mm^2]		
E_1	E_2	E_3	v_{12}	v_{13}	v_{23}	G_{12}	G_{13}	G_{23}
4438.28	1893.28	189.33	0.45	0	0	1090.8	60	60
Plasticity								
Yield strength [N/mm^2]		5.696		Elongation at failure [%]		5.8		MD
Anisotropic parameters								
R_{11}	R_{22}	R_{33}	R_{12}	R_{13}	R_{23}			
1	0.403	0.406	1.105	1	1			

Process simulation

CAD data of the tools were used in explicit numerical simulations, which were executed by means of Abaqus 2021 (Dassault Systémes SE). Paperboard samples were placed in contact with the die. After starting the process, the blank holder first applied force to the sample. In the next step, the die started the deep drawing process by moving into the die.

Mass scaling was used to reduce the simulation time while ensuring that the increased inertial forces did not interfere with the model representing a quasi-static process. The selected element type was C3D8R, an eight-node hexahedral continuum element with reduced integration and enhanced hourglass control. The element sizes were determined by a convergence analysis to ensure that the computation time was not unnecessarily increased while still having a realistic number of wrinkles. The global element size was chosen to be 1 mm, with two elements in the z-direction.

RESULTS AND DISCUSSION

Drawing Depth

Packaging products come in a variety of sizes, as products vary greatly. While the bottom area of the packaging can be adapted easily, the height of the product is often the limiting factor when working with formed papers. Increasing the maximum achievable forming degree is one of the most important goals in paperboard forming research.

Experimental

The drawing depth of the baseline experiments is limited to 40 mm. At this drawing depth, 40% of the paperboards formed without draw beads in the setup used (Fig. 4, a), while none broke at 30 mm. In a process setup with draw beads, the paperboard was stretched more during the forming process. While the draw beads further away from the forming zone had no influence on the drawing depth, the draw beads with a radius of 2 mm led to rupture more frequently than the baseline results. Evaluation of the 3 mm radius showed better results in terms of drawing depth, with 20% of the paperboards still breaking at 40 mm.

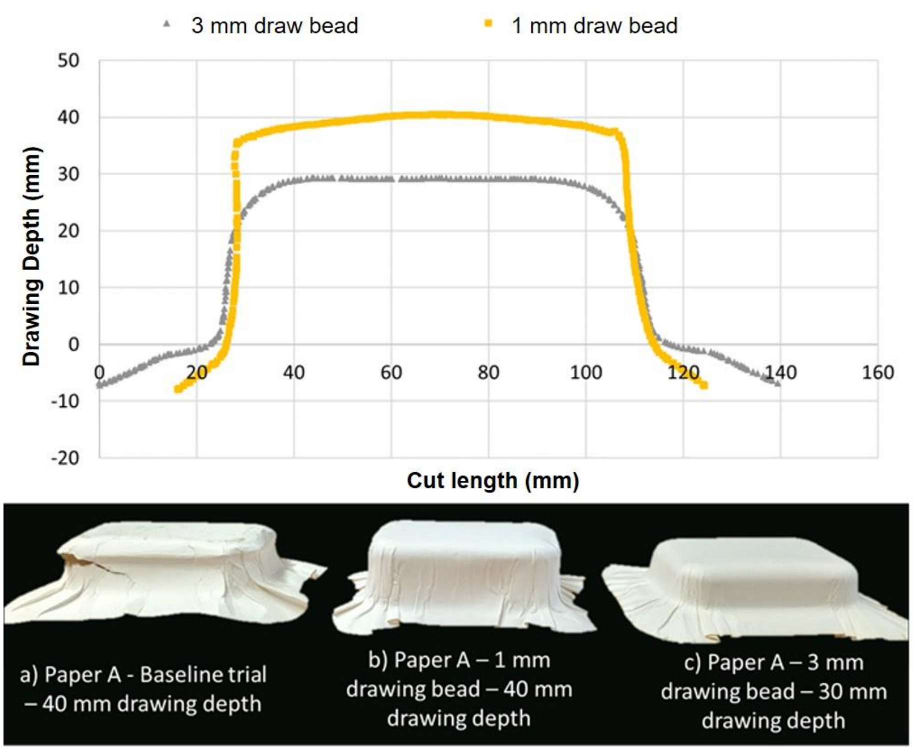

Fig. 4. Drawing depth with different draw beads, cut section measurement on top

It was expected that the 1 mm draw bead would have little impact on the outcome of the experiments. Surprisingly, drawing depths of up to 42 mm were repeatedly achieved with this setup without breakage (Fig. 4). The reason may be that the achievable drawing depth was determined by two factors. On the one hand, the achievable elongation of the material seemed to be highly relevant, which was apparently improved by the guidance through the draw beads. However, the formation of wrinkles and the excess material in the corner radii is an important factor. If the wrinkle density in the corner radii became too high, it seems to have led to an earlier material failure. While the elongation factor was favored by draw beads, the wrinkle density in the corners increased as the draw bead height increased. The 1 mm draw bead offered a compromise between both factors and therefore was able to optimize the process in terms of drawing depth better than higher draw beads.

Regarding bead length, longer beads showed earlier breakage. Since breakage is most likely to occur at the edges of the geometry, the longer beads are likely to compromise the edge area more than the shorter ones, as wrinkles and excess material are compressed more in the corner area. With respect to the elongation of the material due to the draw beads, some additional measurements were made. When identical blanks were deep drawn to the same depth using the same process parameters, with and without a draw bead, the flange length remaining under the blank holder can be compared. The remaining flange length should be longer if a higher material elongation can be achieved, as all blanks have the same size and all geometries have identical drawing depths. The diagram in Fig. 5 shows the comparison of the remaining flange length in MD and CD. The results were recorded both experimentally (see Fig. 5 left) and numerically (see Fig. 5 right). The remaining flange length increased significantly when employing draw beads. In experiments, CD showed an average increase in flange length of 6%, while in MD there was a smaller increase of 1.2%. The higher increase in CD can be explained by the overall higher material ductility, which means that more potential remained in the material throughout the conventional deep drawing process.

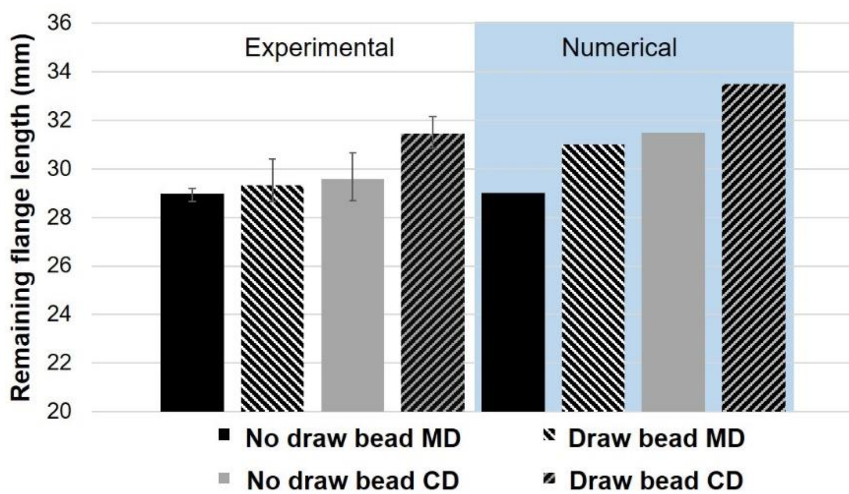

Fig. 5. Comparison of remaining flange depending on draw beads at the same drawing depth

Numerical

Numerical evaluations were performed by defining rupture in relation to the elongation of individual elements. When the critical strain was exceeded, the maximum drawing depth was reached. The baseline experiments showed a maximum drawing depth of 28 mm. The differences to the experimentally achieved 30 mm were based on the necessary assumptions mentioned above, as well as material properties not represented in the model, such as inhomogeneities, air-filled pores, or fiber positions. In the setup with a 3 mm draw bead, a drawing depth of 36 mm was achieved, while the setup with a 1 mm draw bead yielded a drawing depth of 40 mm (Fig. 6). Numerical results were obtained only with the shorter bead length, as the longer beads were shown to fail at critically low drawing depths.

As shown in Fig. 5, the higher elongation of the flange when employing draw beads could also be proven in numerical simulations. The predicted remaining flange length increased when draw beads were used, although the drawing depth remained the same. Overall, the good agreement between the experimental and numerical results showed that the material model can indeed be used to design new tooling concepts. Deviations from the experimental results were higher in CD than in MD. These were probably due to the generally higher strains in CD and thus to a greater effect of the assumptions made. In addition, the properties obtained from the tensile tests and used in the material model were one-dimensional forming properties and did not include the influence of the lower strain in MD on CD.

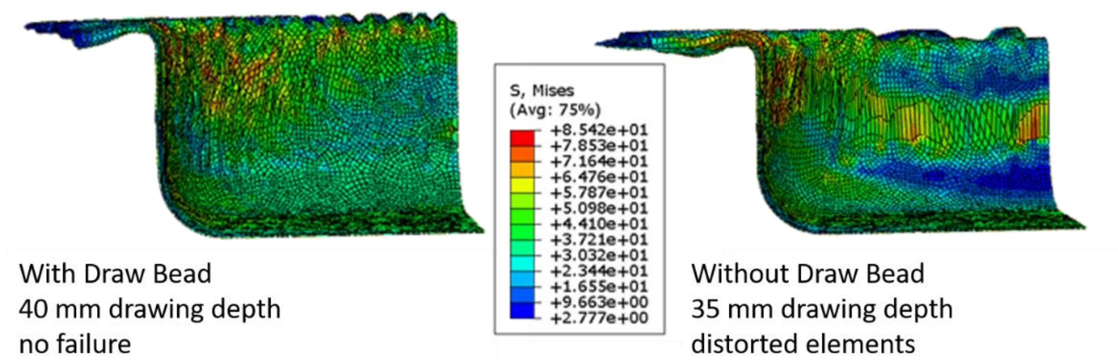

Fig. 6. Results regarding drawing depth in numerical simulations

Figure 6 shows a higher Mises yield stress in the corner area, caused by the high shear load on the material due to wrinkling. In addition, a higher element distortion can be seen in the side wall of the deep drawn results without a draw bead, although it has a lower overall drawing depth.

The corner geometry itself cannot yet be represented quantitatively correctly due to the limited wrinkling caused by the material model. Nevertheless, Fig. 7 shows that without draw beads (foreground, orange) a smaller flange remains at the same drawing depth than with draw beads (background, grey). The left side of Fig. 7 also visualizes the elongation due to the draw bead in the blank holder area.

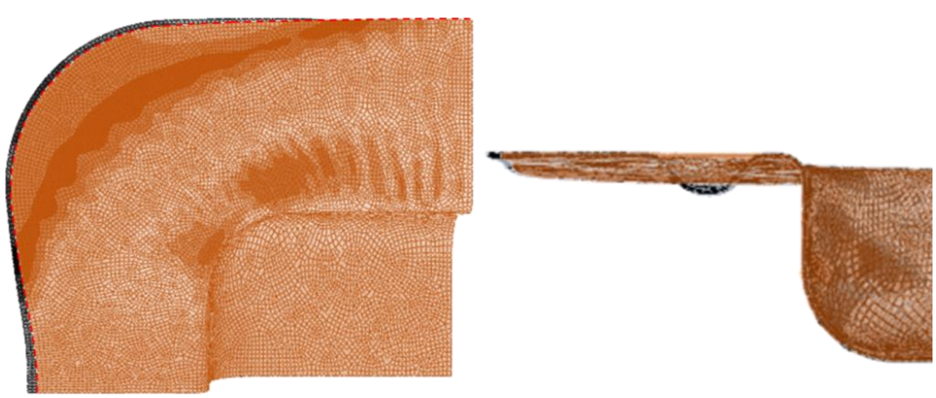

Fig. 7. Comparison of the remaining flange length without (foreground, orange) and with (background, grey) draw beads

Wrinkle Formation

A major goal of this work was to investigate whether introducing draw beads would increase the wrinkle-free distance of the product. This has potential to allow for more surface area on which printing on the package can be placed and read.

Draw beads should help to press the wrinkles well, but also to move them away from the draw beads into the corner radii. To ensure comparability, all results in this section have been recorded at a drawing depth of 30 mm.

Experimental

In both directions, the length of the wrinkle-free section improved for all draw beads, as depicted in Fig. 8. The following aspects emphasize the outcomes:

- Positioned further away from the drawing radius on the outer side, the bead had less effect.
- The longer the draw bead, the greater the effect.
- The higher the bead, the longer the wrinkle-free distance.

These results align with the expectations, as the draw beads displace the wrinkles, and therefore a larger design in both length and height will produce longer wrinkle-free areas.

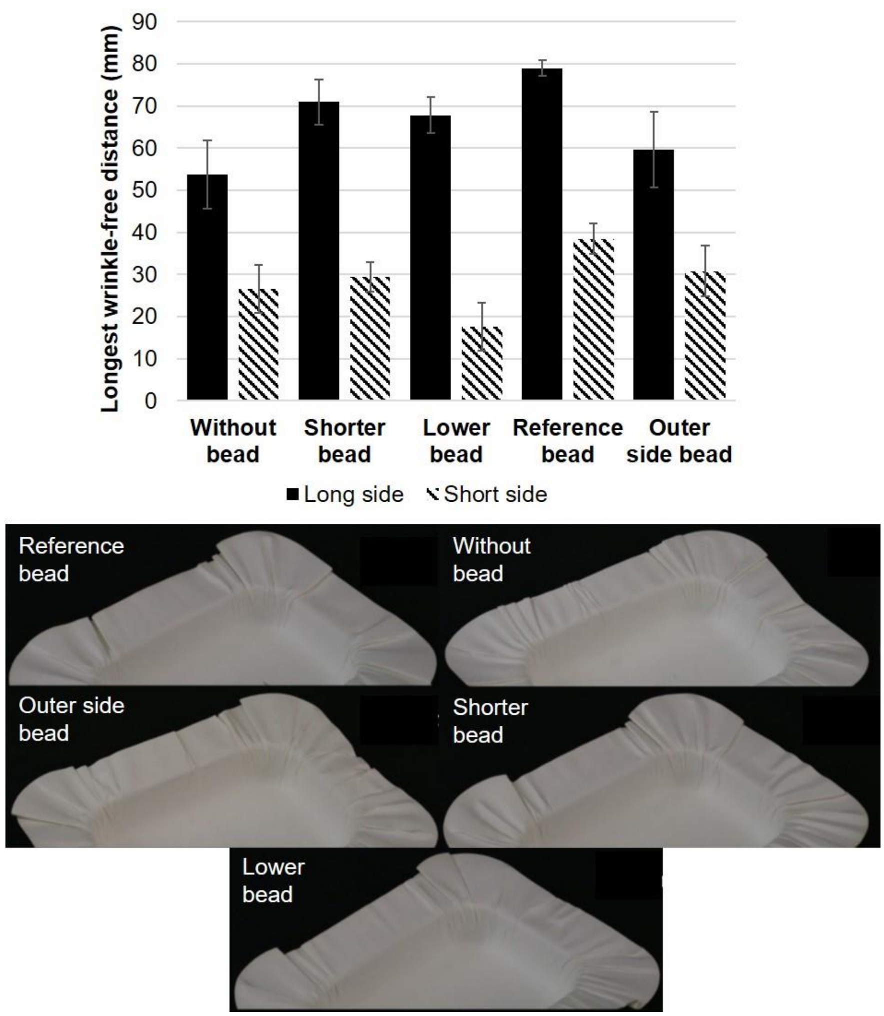

Fig. 8. Difference in the wrinkle free length due to the draw bead geometry

Additionally, the number of wrinkles was analyzed. The results are shown in Fig. 9 and example images are depicted in the lower part of Fig. 8. The trends are as follows:

- The outer side bead results in less wrinkles.
- Longer draw beads result in less wrinkles.
- Higher beads result in less wrinkles.

These results were directly related to the wrinkle-free distances. The longer the wrinkle-free distance, the smaller the wrinkle area. In addition, the higher elongation (Fig. 7) due to the draw beads resulted in less excess material at the same drawing depth, resulting in fewer wrinkles.

However, the outer side bead led to fewer but more voluminous wrinkles. This is because the material is drawn out of the draw bead early in the process. As a result, larger and fewer wrinkles can form to compensate for the excess material. It can also be shown that a lower bead yielded a similar amount of wrinkles as a flat die surface without a draw bead.

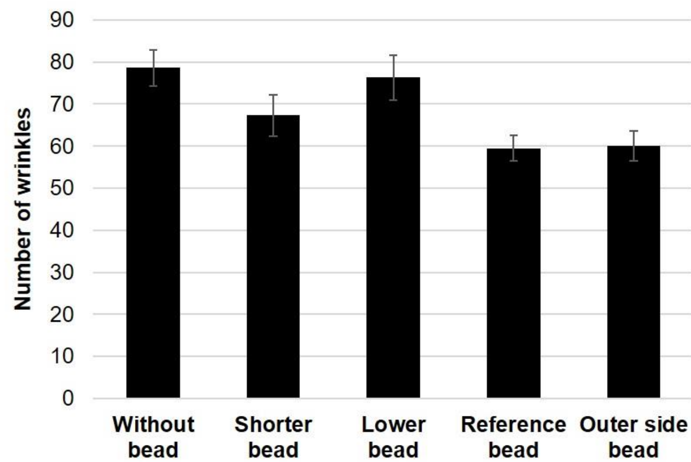

Fig. 9. Differences in the number of wrinkles per half geometry due to draw bead geometry

Numerical

Figure 6 shows the numerical results of the material accumulation in the corner radii. When compared to the experimental results, the representation of wrinkling in numerical simulation is not yet satisfactory.

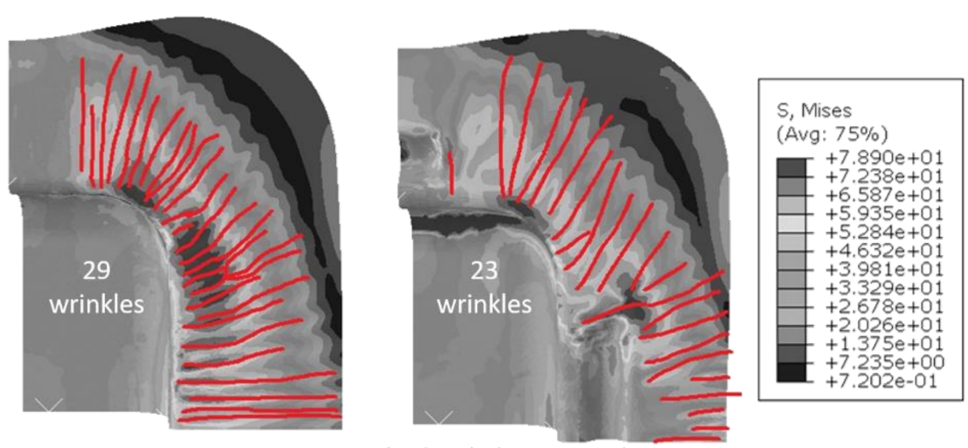

Fig. 10. Number of wrinkles in numerical simulation with no bead (left) and 3 mm reference bead (right)

The numerical simulation generally showed almost no wrinkle-free distances. However, with draw beads, the wrinkles usually appeared behind the bead in the flange area and not in the geometry wall. As shown in Fig. 10, the setup with the reference bead reduced the wrinkle count to 79%, compared to the setup without a draw bead. Experimental studies have shown an average reduction of 76% in the same setup. Thus, while the effect of wrinkle formation itself is not calculated in a fully satisfactory manner, qualitative comparisons of wrinkle counts seem to be admissible. Quantitatively, the total number of wrinkles in the numerical simulation was about a quarter less than in the experimental setup. Furthermore, the wrinkles showed no undercutting but a wavier geometry. This is probably due to the fact that the numerical model does not yet contain the three layers of the real material. With more knowledge about layer buildup, delamination, and interlayer friction, the quantitative results may become more accurate.

CONCLUSIONS

1. Draw beads, especially those with smaller radii, contribute to increasing the drawing depth in paperboard deep drawing processes, potentially mitigating material rupture issues.
2. The presence of draw beads effectively reduces the number of wrinkles formed during deep drawing, particularly influencing the wrinkle-free distance and distribution across the formed part, especially in corner areas.
3. Longer draw beads lead to a greater reduction in wrinkle formation and extend the wrinkle-free distance, suggesting a correlation between draw bead length and wrinkle control.
4. The position of draw beads, particularly when placed closer to the drawing radius, affects the distribution and severity of wrinkles, indicating the importance of strategic placement for optimal wrinkle control.
5. While draw beads show promise in improving process performance, further research is needed to optimize draw bead designs according to local strain and to validate their effectiveness across a broader range of geometries and materials, highlighting avenues for future investigation with, for example, curved beads.

ACKNOWLEDGMENTS

The above research was carried out in the deepening of the project “Paper forming with steam”. The author would like to thank the AiF, the “Federal Ministry of Economic Affairs and Climate Action Germany,” as well as the research association “Kuratorium für Forschung und Technik der Zellstoff- und Papierindustrie e. V”. Further thanks go to StoraEnso for providing test material.

REFERENCES CITED

Directorate General for Environment (2022). "Proposal for a revision of EU legislation on Packaging and Packaging Waste," (https://environment.ec.europa.eu/publications/proposal-packaging-and-packaging-waste_en), accessed 07 March 2024.

DIN 8584-3:2003-09 (2003). "Manufacturing processes forming under combination of tensile and compressive conditions - Part 3: Deep drawing; Classification, subdivision, terms and definitions," Deutsches Institut Fur Normung e.V. (German National Standard), Berlin.

DIN EN ISO 287:2018-03 (2017). "Paper and board - Determination of moisture content of a lot - Oven-drying method," Deutsches Institut Fur Normung e.V. (German National Standard), Berlin.

DIN EN ISO 5270:2022-12 (2022) "Pulps - Laboratory sheets - Determination of physical properties" Deutsches Institut Fur Normung e.V. (German National Standard), Berlin.

European Paper Recycling Council (2021). *Monitoring Report 2021 – European Declaration on Paper Recycling 2021-2030*, Brussels.

Garat, W., Le Moigne, N., Corn, S., Beaugrand, J., and Bergeret, A. (2020). "Swelling of natural fibre bundles under hygro- and hydrothermal conditions: Determination of hydric expansion coefficients by automated laser scanning," *Composites Part A Applied Science and Manufacturing* 131, article 105803. DOI: 10.1016/j.compositesa.2020.105803

Hauptmann, M. Kaulfürst, S., and Majschak, J.-P. (2016). "Advances on geometrical limits in deep drawing process of paperboard," *BioResources* 11(4), 10042-10056. DOI: 10.15376/biores.11.4.10042-10056

Huang, H., and Nygårds, M. (2010). "A simplified material model for finite element analysis of paperboard creasing," *Nordic Pulp & Paper Research Journal* 25(4), 502-509. DOI: 10.3183/npprj-2010-25-04-p502-509

Hussein, N. Z., Ameen, H. A., and Saleh, A. H. (2020). "Effect of the location of draw bead and its profile in cylindrical cup forming," in: *3rd International Conference on Sustainable Engineering Techniques (ICSET 2020)*, Baghdad, Iraq. DOI: 10.1088/1757-899X/881/1/012054

Huttel, D. (2015). *Wirkmedienbasiertes Umformen von Papier*, Shaker Verlag, Berichte aus Produktion und Umformtechnik. ISBN: 9783844038118

Jessen, N., Schetle, M., and Groche, P. (2022), "Numerical analysis of the deep drawing process of paper boards at different humidities," in: *Proceedings of the 12th Congress of the German Academic Association for Production Technology (WGP)*, pp. 131-141. DOI: 10.1007/978-3-031-18318-8_14

Lev, R., Tanninen, P., Lyytikäinen, J., and Leminen, V. (2023). "Converting and its effects on barrier properties of coated packaging materials: A Review," *BioResources* 18(4), 8707-8728, DOI: 10.15376/biores.18.4.Lev

Murali, G. A., Gopal, B. M., and Rajadurai, A. (2010). "Analysis of influence of draw bead location and profile in hemispherical cup forming," *International Journal of Engineering and Technology* 2(4), 356-360. DOI: 10.7763/IJET.2010.V2.147

Papadia, G., Del Prete, A., Manisi, B., and Anglani, A. (2010). "Blank shape optimization in sheet metal hydromechanical deep drawing," *International Journal of Material Forming* 3, 291-294. DOI: 10.1007/s12289-010-0764-6

Pfeiffer, M., and Kolling, S. (2019). "A non-associative orthotropic plasticity model for paperboard under in-plane loading," *International Journal of Solids and Structures* 166. DOI: 10.1016/j.ijsolstr.2019.02.012

Safwa, M., Yeddu, H. K., and Leminen, V. (2024). "Modeling of the thermoforming process of paperboard composites for packaging," *BioResources* 19(2), 2120-2134, DOI: 10.15376/biores.19.2.2120-2134

Two Sides UK (2020). *European Packaging Preferences 2020 - A European Study of Consumer Preferences, Perceptions, and Attitudes towards Packaging*, Daventry, UK.

VDI 3141:2000-01 (2000). "Lock steps and draw beads in large forming dies"

Vishtal, A., and Retulainen, E. (2012). "Deep drawing of paper and paperboard: The role of material properties," *BioResources* 7(3), 4424-4450. DOI: 10.15376/biores.7.3.4434-4450

Wallmeier, M., Hauptmann, M., and Majschak, J. (2014). "New methods for quality analysis of deep-drawn packaging components from paperboard," *Packaging Technology and Science* 28(2), 91-100. DOI: 10.1002/pts.2091

Wallmeier, M., Hauptmann, M., and Majschak, J. P. (2016). "The occurrence of rupture in deep drawing of paperboard," *BioResources* 11(4), 4688-4704. DOI: 10.15376/biores.11.2.4688-4704

Article submitted: June 7, 2024; Peer review completed: June 22, 2024; Revised version received: July 19, 2024; Accepted: December 4, 2024; Published: December 12, 2024.
DOI: 10.15376/biores.20.1.1399-1412